



# INTELLIGENT SYSTEM FOR THE DETECTION OF IRON STAIN ON COFFEE GROWING LEAVES

Ferley Medina Rojas<sup>1</sup>, Juan A. Castro Silva<sup>1</sup> and Faiber Robayo Betancourt<sup>2</sup>

<sup>1</sup>Department of Software Engineering, Faculty of Engineering, Surcolombiana University, Neiva, Huila, Colombia

<sup>2</sup>Department of Electronic Engineering, Faculty of Engineering, Surcolombiana University, Neiva, Huila, Colombia

E-Mail: [ferley.medina@usco.edu.co](mailto:ferley.medina@usco.edu.co)

## ABSTRACT

The iron stain is a disease caused by the fungus *Cercospora coffeicola* Berk and Cooke, attacks coffee leaves and fruits in all stages of development of the plant. This article proposes an intelligent system for iron stain detection. The model captures images to reduce the size, increases the data of the data set, segmentation to separate the object of interest from the background, then extracts the study characteristics of the image to be recognized, interpreted and detected in the last classification stage. The proposed system has an effectiveness of 77.32% when detecting the iron stain on coffee leaves with a data set of 2800 images of which, 1400 has the disease and 1400 do not have it. The proposed system helps farmers to control iron stain early by contributing to a healthy crop that generates good crop yield.

**Keywords:** iron stain, intelligent system, data augmentation.

## 1. INTRODUCTION

The iron stain disease that attacks the leaves and fruits of coffee in all states can affect up to 30% of the crop (CONSUELO MONTES R., 2012). Conventional methods that are currently used for the diagnosis and identification of diseases that affect coffee cultivation in Colombia depend on traditional techniques such as observation at a glance by coffee growers, experts, or professionals trained in the subject. The slow, tedious and costly process increases the production costs of the crop and reduces its yield.

However, in Colombia, a study was conducted that aimed to use image processing to determine the severity of iron stain on coffee leaves. A program was developed in Matlab 5.3, which allows knowing precisely and quickly the area of the coffee leaf and the area affected by the diseases (Guzmán P., Gómez G., O., C.A., & Oliveros T., 2003).

On the other hand, Aristizábal Galvis (Aristizábal G., 2017), implemented a methodology based on computer vision to detect diseases in fruit crops at an earlier stage, using a supervised learning method. Descriptors based on RGB, TSL and Lab color histograms were used. The average yield of 79.91% ± 10.50% in banana crops, 98.72% ± 1.81% in tomato crops, and 70.88% ± 5.76% for blackberry cultivation. Concluding that RGB color descriptors present greater efficiency to the rest of the descriptors used.

Another case study was carried out in Ethiopia, its main objective was the recognition of diseases of coffee rust and wilting on the leaves of the plant; using image recognition and machine learning techniques. Different classifiers were trained: ANN, KNN, RBF, and a combination of SOM and RBF. The latter presented the highest accuracy compared to the other classifiers, obtaining a performance of 90.07% (Mengitsu, Alemayehu, & Mengitsu, 2016).

Therefore, the intelligent model is based on computer vision, it includes a set of techniques to obtain, process, analyze and recognize real-world images, with the

aim of transforming them into their numerical representation so that they can be treated by a computer. One of these techniques, the detection of objects, which gives a machine the ability to detect instances of various kinds, such as people, animals, buildings and many more, in an image or video (Papageorgiou & Poggio, 2000). An object detection algorithm in images implies the identification of what type is the object of interest. The location within the image, get the coordinates of the detection window that contains it (Girshick, Donahue, Darrel, & Malik, 2014).

The proposed solution uses deep learning algorithms with a 77.32% effectiveness in the diagnosis of iron stain disease. In chapter 2, the methodology used will be discussed. In chapter 3, the results and finally the conclusions and recommendations for future work are shown.

## 2. MATERIALS AND METHODS

### 2.1 Obtaining images

The images were captured in an uncontrolled light environment with RGB color space, at a focal length of 15 centimeters with the camera of a Samsung Galaxy S7 Edge mobile device, which has a Samsung SM-G935F camera, opening of F: 1.7, focal length 4.2 mm, exposure between 1/500 to 1/600 seconds, ISO 50, resolution of 3024x4032.

Figure-1 shows a captured image of size 3024 x 4032, in the beam of the coffee leaf, it presents infection with iron stain.



Figure-1. Original Image Obtained.

## 2.2 Re-size

Re-size is a geometric transformation in image processing, which reduces or increases the number of pixels in an image while retaining the most relevant information to maintain the characteristics of the original image (Dharavath, Talukdar, & Laskar, 2014). The procedure used is based on the Nearest Neighbor interpolation algorithm, and simply determines the closest pixel of the surroundings, and assumes its intensity value.

When you want to scale to a larger image, there is the question of what will be the color of the new pixels that are between the original pixels. However, when you want to scale to a smaller image, the question becomes what the color of the remaining pixels will be, because in this case, it involves the reduction of pixels and this translates into an unrecoverable loss of information (GF, S, & L). To reduce the image by a factor  $n$ , the inverse principle of the nearest neighbor is to choose a pixel from those that have the same intensity.

Figure-2 shows the rescaling of an image of  $9 \times 9$  pixels to a  $2 \times 2$ . The proportion of the new image is given by equation 1.

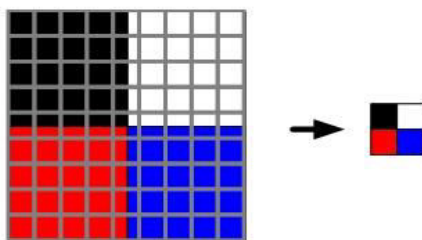


Figure-2. Re-size scheme of an image.

$$w_2, h_2 \neq 0 \begin{cases} x_{ratio} = \frac{w_1}{w_2} \\ y_{ratio} = \frac{h_1}{h_2} \end{cases} \quad (1)$$

where  $w_1, h_1$  are the width and length of the original image and  $w_2, h_2$  the width and length of the rescaled image.

This method was used to reduce the size of the data set images that were from  $3024 \times 4032$  pixels to

$350 \times 350$  pixels for their high computational cost in processing. The language used in the programming of this project in Python. The resize was performed with the implementation of the `imutils` library and its `resize` method, receives as parameters the initial image, width, and height that you want to apply to it as shown in equation 2.

$$\mathbf{H} = \text{resize}(\mathbf{H}, (w, l)) \quad (2)$$

where  $w$  is the width of the image,  $l$  is the length of the image and  $\mathbf{H}$  is the input image.

## 2.3 Segmentation

Segmentation is a process that allows you to divide an image into several homogeneous and disjoint zones or regions, in terms of a set of pixel characteristics that allow you to discriminate some regions from others (Nikhil & Sankar, 1993). The segmentation technique used is based on Canny's edge detection algorithm, which first performs a noise reduction to the image by applying a Gaussian filter. The Gaussian filter of size  $(2k + 1) \times (2k + 1)$  is given by equation 3.

$$H_{i,j} = \frac{1}{2\pi\sigma^2} \exp\left(-\frac{(i - (k + 1))^2 + (j - (k + 1))^2}{2\sigma^2}\right) \quad (3)$$

$$1 \leq i, j \leq (2k + 1)$$

Where  $i$  refers to the position of the pixel in the rows of the image matrix and  $j$  in the columns.  $k$  is the size of the filter as shown in equations 4 and 5. If the filter is applied, a smoothed version of the image is obtained, the smaller the size of the filter, the less visible the smoothing will be. Once the noise in the image is reduced, the procedure known as gradient calculation is performed, by implementing Sobel filters both horizontally and vertically. This process is done to detect the intensity and direction of edges, equations 4 and 5.

$$K_x = \begin{pmatrix} -1 & 0 & 1 \\ -2 & 0 & 2 \\ -1 & 0 & 1 \end{pmatrix} \quad (4)$$

$$K_y = \begin{pmatrix} 1 & 2 & 1 \\ 0 & 0 & 0 \\ -1 & -2 & -1 \end{pmatrix} \quad (5)$$

$K_x$  and  $K_y$  are the Sobel filters applied by convolution with the smoothed image obtaining  $I_x, I_y$ . The magnitude and direction of the gradient are calculated using equations 6 and 7.

$$|G| = \sqrt{I_x^2 + I_y^2} \quad (6)$$

$$\theta_{x,y} = \arctan\left(\frac{I_y}{I_x}\right) \quad (7)$$



Once the edges are detected, refinement is carried out with the suppression of pixels outside the edge and the application of a hysteresis threshold. The segmentation technique was implemented in order to separate the area or object of interest for the extraction of characteristics, which corresponds to the coffee leaf as shown in Figure-3.



Figure-3. Segmented image.

#### 2.4 Data augmentation

Data augmentation is a technique that is used in image processing to artificially increase the size of a data set by creating modified versions of images from the initial dataset (Inoue, 2018). The Random Rotation Augmentation process was implemented, which rotates the original image clockwise, taking into account the adjustment of the image frame to avoid losing areas that may be outside the original frame when rotated.

The OpenCV library for Python provides scaled rotation with an adjustable rotation center so that it can be rotated where preferred. The rotation is given by applying the 2x3 transformation matrix M as shown in equation 8.

$$\begin{bmatrix} \alpha & \beta & (1 - \alpha) * \text{center.x} - \beta * \text{center.y} \\ -\beta & \alpha & \beta * \text{center.x} + (1 - \alpha) * \text{center.y} \end{bmatrix} \quad (8)$$

Where  $\alpha = \text{scale} * \cos \theta$ ,  $\beta = \text{scale} * \sin \theta$  and  $\theta$  is the angle of rotation of the image. The new image is given by equation 9.

$$H_r(x, y) = H(M_{1,1}x + M_{1,2}y + M_{1,3} + M_{2,1}x + M_{2,2}y + M_{2,3}) \quad (9)$$

The implementation of the imutils library and the rotate\_bound method which receives as parameters the image and the angle of rotation, as shown in equation 10.

$$H = \text{imutils.rotate\_bound}(H, \theta) \quad (10)$$

Applying the technique, the following results were obtained corresponding to the number of images that make up the dataset, according to Table-1 composed of 1400 images with iron stain and 1400 without iron stain for a balanced dataset.

Table-1. Dataset Data Augmentation.

Categories	Originals	Results
Iron stained leaves (beam and underside)	448	1400
Ironless stain leaves	129	1400

#### 2.5 Model training

The ResNet50 convolutional neural network architecture is implemented in the classification of the images. The parameters used are shown in Table-2.

Table-2. Training parameters.

Parameters	Description / Values
$H_{1..n}$	Training images
$B_{1..n}$	Validation Images
Image size	350 x 350
batch_size	64
Learning_rate	0.001
epochs	100
Class_mode	“categorical”

The training algorithm uses the following:  $\text{model.fit\_generator}(H_{1..n}, 64, \text{categorical}, 100, B_{1..n})$  function to allow layers to be added sequentially.

The model was trained with four sets, 80% of each for training and 20% for validation. The first and the second without segmentation, with iron stain and the other without iron stain. The third and fourth with segmentation, with iron stain and the other without iron stain as seen in Table 3.

Table-3. Dataset used for training and model validation.

Categories	Training	Validation
Iron stained leaves (not segmented)	1120	280
Ironless stain leaves (not segmented)	1120	280
Iron stained leaves (segmented)	1120	280
Ironless stain leaves (segmented)	1120	280

### 3. RESULTS AND DISCUSSIONS

Three simulations of the model were executed. The first was made with non-segmented images containing sheets with iron stain and no iron stain, as a result, an overtraining was obtained. The second with segmented images containing sheets with iron stain and no iron stain, as a result, an overtraining was obtained. In the latter, a



combination of all images was made in equal parts, leaves with iron stain and without iron stain, segmented and non-segmented, achieving a classification of 77.32% as shown in Table-4. An adequate percentage to detect iron stain disease in coffee crops at an early age.

**Table-4.** Simulation Results.

Simulations	Categories	Cantidad	Results
1	Iron stained leaves (not segmented)	1400	overfitting
	Ironless stain leaves (not segmented)	1400	
2	Iron stained leaves (segmented)	1400	overfitting
	Ironless stain leaves (segmented)	1400	
3	Iron stained leaves (not segmented)	700	77.32%
	Ironless stain leaves (not segmented)	700	
	Iron stained leaves (segmented)	700	
	Ironless stain leaves (segmented)	700	

#### 4. CONCLUSIONS

The classification obtained in the model achieved a result of 77.32% with deep learning techniques, adequate value according to the dataset conditions. Besides, coffee growers can detect the disease at an early age and avoid reducing the crop.

The dataset must be balanced, where each category has the same number of images so that the classifier does not show a preference for a particular category. The training images must be different from the validation ones, otherwise, the classifier may tend to over-train.

Finally, the training dataset must contain images that group all the representative characteristics of the disease, in each of its stages of development and different conditions.

#### REFERENCES

Aristizábel G., C. 01 de 01 de 2017. Evaluación de un método de aprendizaje supervisado para la detección de las enfermedades, Antracnosis y Phytophthora Infestans en cultivos de fruta de Risaralda. Obtenido de Universidad Tecnológica de Pereira.

Consuelo M. R., Oscar Armando P. & Roberto Amilcar C. 2012. Infestación e incidencia de broca, roya y. Biotecnología en el Sector Agropecuario y Agroindustrial. 10(1): 98-108.

Dharavath K., Talukdar F. A. & Laskar R. H. 2014. Improving face recognition rate with image preprocessing. Indian Journal of Science and Technology. Vol. (1170-1175).

GF W., S, L. & L G. 2006. United stated Patente nº 7,142,729.

Girshick R., Donahue J., Darrel T. & Malik J. 2014. Rich feature hierarchies for accurate object detection and semantic segmentation. CVPR2014 (pp. 1-8). Columbus: Computer Vision Foundation.

Guzmán P., O., Gómez G., E. O., O., R., C.A, & Oliveros T., C. 2003. Utilización del procesamiento de imágenes para determinar la severidad de la mancha de hierro en las hojas de café. Cenicafé. 54(3): 258-265.

Inoue H. 2018. Data augmentation by pairing samples for images classification. Computer Science. 1101-1105.

Mengitsu A., Alemayehu D. & Mengitsu S. 2016. Ethiopian Coffe Plant Diseases Recognition Based on Imaging and Machine Learning Technique. International Journal of Database Theory and Application. 9: 79-88.

Nikhil R. P. & Sankar K. P. 1993. A review on image segmentation techniques. Pattern Recognition. 26(9): 1277-1294.

Papageorgiou C. & Poggio T. .-3. 2000. A trainable system for object detection. International Journal of Computer Vision. 38(1): 15-33.